This is a repository copy of *Evaluation of Sydnone-Based Analogs of Combretastatin A-4 Phosphate (CA4P) as Vascular Disrupting Agents for Use in Cancer Therapy*.

White Rose Research Online URL for this paper:
http://eprints.whiterose.ac.uk/137134/

Version: Accepted Version

Article:
Harrity, J.P.A., Brown, A., Holmes, T. et al. (3 more authors) (2018) Evaluation of Sydnone-Based Analogs of Combretastatin A-4 Phosphate (CA4P) as Vascular Disrupting Agents for Use in Cancer Therapy. ChemMedChem. ISSN 1860-7179

https://doi.org/10.1002/cmdc.201800567

Reuse
Items deposited in White Rose Research Online are protected by copyright, with all rights reserved unless indicated otherwise. They may be downloaded and/or printed for private study, or other acts as permitted by national copyright laws. The publisher or other rights holders may allow further reproduction and re-use of the full text version. This is indicated by the licence information on the White Rose Research Online record for the item.

Takedown
If you consider content in White Rose Research Online to be in breach of UK law, please notify us by emailing eprints@whiterose.ac.uk including the URL of the record and the reason for the withdrawal request.

eprints@whiterose.ac.uk
https://eprints.whiterose.ac.uk/

Evaluation of Sydnone-Based Analogs of Combretastatin A-4 Phosphate (CA4P) as Vascular Disrupting Agents for Use in Cancer Therapy

Andrew W. Brown,[a,b] Toby Holmes,[b] Matthew Fisher,[b] Gillian M. Tozer,*[b] Joseph P. A. Harrity,*[a] and Chryso Kanthou*[b]

[a] Dr. A. W. Brown, Prof. J. P. A. Harrity
Department of Chemistry
The University of Sheffield
Dainton Building, Brook Hill
Sheffield S3 7HF, (U.K.)
E-mail: j.harrity@sheffield.ac.uk

[b] Dr. T. Holmes, Mr. M. Fisher, Prof. G. M. Tozer, Dr. C. Kanthou
Department of Oncology & Metabolism
The University of Sheffield
The Medical School, Beech Hill Road
Sheffield S10 2RX, (U.K.)

Supporting information for this article is given via a link at the end of the document.

Abstract: The combretastatins have attracted significant interest as small molecule therapies for cancer due to their ability to function as vascular disrupting agents. We have successfully prepared a range of combretastatin analogs that are based on a novel sydnone heterocycle core, and their potential as tubulin binders has been assessed *in vitro* and *in vivo*. The most potent candidate was found to disrupt microtubules and affect cellular morphology at sub-micromolar levels. Moreover, it was found to bind reversibly to tubulin and significantly increase endothelial cell monolayer permeability, in a similar manner to combretastatin A4. Surprisingly, the compound did not exhibit efficacy *in vivo*, possibly due to rapid metabolism.

Introduction

A growing area of research has focussed on targeting the blood supply of tumors.[1,2] A tumor relies on a functional blood vessel network to grow and survive,[3] hence tumor blood vessels are attractive targets for anticancer drugs.[4] Of the current vascular targeting methods, vascular disrupting agents (VDAs) possess particularly desirable characteristics. By definition, VDAs cause the rapid and selective collapse of tumor blood vessels, resulting in extensive necrotic cell death within the tumor.[1] Most VDAs fall into two categories; analogs of flavone acetic acid (FAA)[5,6] and microtubule depolymerizing agents.[4] Of these, microtubule depolymerizing agents have received the most attention. Indeed, the classical tubulin binding agent – colchicine (Figure 1) – has been known to damage tumor blood vessels since the 1930s.[7] However, colchicine is too toxic to use in this regard.[8] Structurally related to colchicine, the combretastatins were isolated from the Cape Bush Willow tree *Combretum caffrum* and exhibited great promise as VDAs.[9-11] The most active compound isolated – combretastatin A-4 (CA4) – instigated tumor blood vessel disruption within minutes at well below the maximum tolerated dose (MTD).[12] To aid water solubility, it was developed into the prodrug, disodium combretastatin A-4 3-*O*-phosphate (CA4P).[13] The higher toxicity of colchicine relative to CA4 is thought to arise from differences in binding to the β-tubulin subunit. Colchicine is thought to bind pseudo-irreversibly leading to further downstream toxic effects, whereas CA4 binds reversibly.[14] The low toxicity and exciting activity of CA4P resulted in its evaluation as an anticancer agent in clinical trials as single agent and more recently in combination with cytarabine.[15,16]

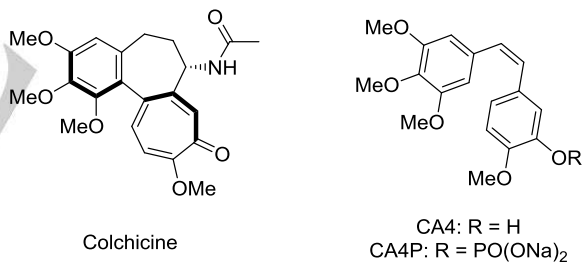

Colchicine

CA4: R = H
CA4P: R = $PO(ONa)_2$

Figure 1. Structures of colchicine and CA4P.

Despite continued interest in CA4P as a clinical candidate, there are a number of underlying issues with the compound. In particular, the *cis* geometry of the alkene linker is fundamental to its activity, with the *trans* isomer exhibiting essentially zero activity.[17] This issue is further compounded by the propensity of stilbenes to undergo *cis-trans* isomerization in heat, light and protic media.[18] A potential solution is the replacement of the alkene linker with a heterocycle.[19-24] Such a strategy essentially "fixes" the linker geometry and prevents loss of activity through metabolic isomerization. Although a number of significant contributions have been made in the field of rigid combretastatin analogs, sydnone analogs have yet to be studied. Sydnones are unusual but stable dipolar compounds, and are referred to as mesoionic (Figure 2).[25] We have had a significant interest in the chemistry of sydnones for a number of years,[26-29] but until now have not studied their potential as pharmacological agents. In light of our development of a robust and versatile route to synthesize diarylsydnones,[30] we sought here to prepare a

number of novel sydnone-bridged combretastatin analogs and assess their efficacy as VDAs.

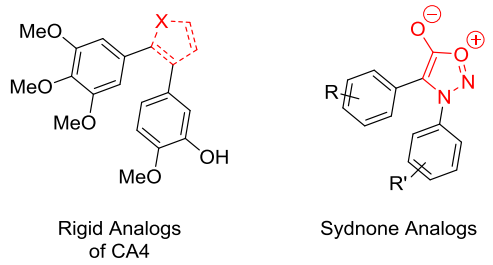

Figure 2. Sydnone-based rigid analogs of CA4.

Results and Discussion

Chemistry

A range of diarylsydnones were readily prepared using direct arylation methodology developed in our laboratories (Table 1).[30] Previous studies have indicated that the 3,4,5-trimethoxyphenyl ring is key to the activity of combretastatin analogs.[31,32] Therefore, we focussed the majority of our efforts into the synthesis of analogs containing this motif on both the *N*3 (entries 1-10) and *C*4 (entries 11-13) of the sydnone. We were also able to prepare an analogue of AVE 8062, a former Sanofi Aventis clinical candidate, in excellent yield (Entry 9).[4] Direct analogs of CA4 were also readily prepared, without the use of protecting groups (Entries 10 and 11).

Biological Evaluation

Although a significant number of combretastatin analogs have been developed over the years, a general *in vitro* method for assessing their efficacy has proved elusive. A large number of reports focus on the direct activity of the compounds against cancer cells.[33] Studies from our laboratories have previously shown that although *in vitro* CA4P targets tumor cells and inhibits their proliferation, *in vivo* it is predominantly its vascular effects that are responsible for killing tumor cells by necrosis.[34] Therefore, assays involving direct action on cancer cells may not necessarily predict the vascular disruptive capabilities of a compound. Instead, VDA effects on the microtubule cytoskeleton of endothelial cells (the primary target of VDAs) and subsequent changes in cell morphology are thought to be integral to their therapeutic efficacy.[35] Indeed, recently, we have shown that assays using endothelial cells provided a good insight into the activity CA4 analogs that translated into *in vivo* efficacy.[36]

Initial Screens

Initially, compounds were studied for anti-proliferative activity against endothelial cells.

Several *N*-(3,4,5-trimethoxyphenyl) (TMP) compounds had either low activity or were completely inactive in the assay (Table 2, entries 1-8). Nanomolar activity was achieved with more conventional analogs of CA4 (entries 9, 10 and 11). It was interesting to note that aniline **9** was more active than direct CA4 analogue **10**. More interesting still was that structural isomer **11** was an order of magnitude higher in activity than **10** (entry 11). Indeed, compounds bearing the TMP unit at the sydnone *C*4 exhibited higher activity than their *N*3-substituted isomers **– 12** vs **7** (entry 12 vs 7) and **13** vs **1** (entry 13 vs 1). All further diarylsydnones showed little to no activity (entries 14-20). As controls, both CA4P and colchicine were used in the assay and were found to be potent at low nanomolar concentrations, as expected. Importantly, derivatisation of **11** to the highly water-soluble disodium phosphate salt **23** maintained activity, indicating that the phosphate was rapidly cleaved in media containing serum. The most active compounds from the initial screens are depicted in Figure 3.

Table 1. Synthesis of sydnone-based analogs of CA4.

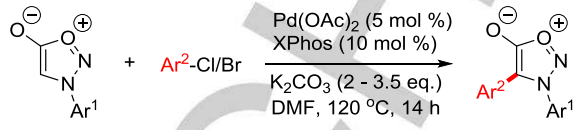

Entry	Compound	Ar^1	Ar^2	Yield
1	**1**	3,4,5-$MeOC_6H_2$	4-$MeOC_6H_4$	73%
2	**2**	3,4,5-$MeOC_6H_2$	2-$MeOC_6H_4$	71%
3	**3**	3,4,5-$MeOC_6H_2$	Ph	81%
4	**4**	3,4,5-$MeOC_6H_2$	4-MeC_6H_4	96%
5	**5**	3,4,5-$MeOC_6H_2$	3-$NO_2C_6H_4$	90%
6	**6**	3,4,5-$MeOC_6H_2$	2-Thiophenyl	81%
7	**7**	3,4,5-$MeOC_6H_2$	4-$EtOC_6H_4$	92%
8	**8**	3,4,5-$MeOC_6H_2$	2-ClC_6H_4	73%
9	**9**	3,4,5-$MeOC_6H_2$	3-H_2N-4-$MeOC_6H_3$	91%
10	**10**	3,4,5-$MeOC_6H_2$	3-HO-4-$MeOC_6H_3$	81%
11	**11**	3-HO-4-$MeOC_6H_3$	3,4,5-$MeOC_6H_2$	47%
12	**12**	4-$EtOC_6H_4$	3,4,5-$MeOC_6H_2$	76%
13	**13**	4-$MeOC_6H_4$	3,4,5-$MeOC_6H_2$	71%
14	**14**	4-$MeOC_6H_4$	4-$MeOC_6H_4$	79%
15	**15**	4-$MeOC_6H_4$	Ph	83%
16	**16**	4-$MeOC_6H_4$	2-Thiophenyl	89%
17	**17**	4-$MeOC_6H_4$	2-ClC_6H_4	94%
18	**18**	4-$MeOC_6H_4$	3-$NO_2C_6H_4$	85%
19	**19**	4-$EtOC_6H_4$	4-MeC_6H_4	77%
20	**20**	Ph	4-MeC_6H_4	83%

Table 2. Values for growth inhibition of HUVECs by sydnone anologs versus CA4P and colchicine.

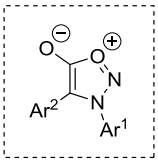

Entry	Compound	Ar^1	Ar^2	GI_{50}[a]
1	**1**	3,4,5-$MeOC_6H_2$	4-$MeOC_6H_4$	>20 μM
2	**2**	3,4,5-$MeOC_6H_2$	2-$MeOC_6H_4$	>20 μM
3	**3**	3,4,5-$MeOC_6H_2$	Ph	>20 μM
4	**4**	3,4,5-$MeOC_6H_2$	4-MeC_6H_4	>20 μM
5	**5**	3,4,5-$MeOC_6H_2$	3-$NO_2C_6H_4$	>20 μM
6	**6**	3,4,5-$MeOC_6H_2$	2-Thiophenyl	>20 μM
7	**7**	3,4,5-$MeOC_6H_2$	4-$EtOC_6H_4$	4.1±0.2 μM
8	**8**	3,4,5-$MeOC_6H_2$	2-ClC_6H_4	>20 μM
9	**9**	3,4,5-$MeOC_6H_2$	3-H_2N-4-$MeOC_6H_3$	315±9 nM
10	**10**	3,4,5-$MeOC_6H_2$	3-HO-4-$MeOC_6H_3$	526±14 nM
11	**11**	3-HO-4-$MeOC_6H_3$	3,4,5-$MeOC_6H_2$	36±2 nM
12	**12**	4-$EtOC_6H_4$	3,4,5-$MeOC_6H_2$	1.5±0.05 μM
13	**13**	4-$MeOC_6H_4$	3,4,5-$MeOC_6H_2$	336±12 nM
14	**14**	4-$MeOC_6H_4$	4-$MeOC_6H_4$	>20 μM
15	**15**	4-$MeOC_6H_4$	Ph	2.3±0.1 μM
16	**16**	4-$MeOC_6H_4$	2-Thiophenyl	>20 μM
17	**17**	4-$MeOC_6H_4$	2-ClC_6H_4	5.2±0.3 μM
18	**18**	4-$MeOC_6H_4$	3-$NO_2C_6H_4$	13.3±0.8 μM
19	**19**	4-$EtOC_6H_4$	4-MeC_6H_4	>20 μM
20	**20**	Ph	4-MeC_6H_4	>20 μM
21	CA4P	--	--	8±0.5 nM
22	Colchicine	--	--	25±2 nM
23	**23**	3-[$(NaO)_2OPO$]-4-$MeOC_6H_3$	3,4,5-$MeOC_6H_2$	51±3 nM

[a]. HUVECs were plated in 96-multiwell plates and 24 h later they were treated with drug or vehicle. At 72 h after treatment, cells were fixed and stained with 1% crystal violet, washed and the dye was solubilised in 10% acetic acid. Viable cells were quantified by the absorbance at 590 nm. Results are a mean of 3 independent experiments ± SEM.

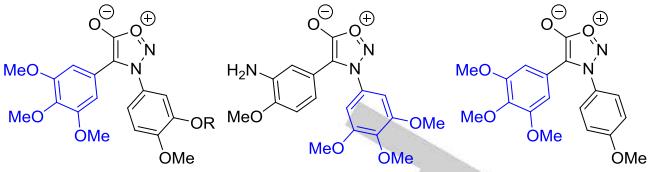

11: R = H: 41 nM
23: R = $PO(ONa)_2$: 51 nM

9: 315 nM

13: 336 nM

Figure 3. Most active sydnone analogs from initial screening.

Immunofluorescence Studies

Although proliferation studies on endothelial cells are a useful indicator of potential VDA activity, they do not provide information on the mechanism of inhibition, in particular with respect to tubulin binding. Indeed, the vascular damaging effects of VDAs are unlikely to be due to their anti-proliferative activity. Instead, effects on cell shape and morphology, and junction integrity instigated on a much shorter timescale (within minutes) are the most likely cause of VDA-mediated vascular collapse.[35,37] A number of previous studies have used tubulin depolymerisation assays to support a tubulin binding mode of action.[32,38] Although useful in providing evidence of tubulin binding, the assays are expensive and require high concentrations of drug for an effect to be observed. An alternative approach to supplement proliferation studies is to visualize the cell cytoskeleton by immunofluorescence. This allows drug-induced changes in shape and morphology to be observed and effects on specific cellular structures to be monitored. The vascular disruptive effects of CA4 are thought to arise from microtubule disruption, accompanied by changes in cell shape and morphology brought about by remodelling of the actin cytoskeleton.[35] Therefore, endothelial cells in culture were stained using using phalloidin which stains actin filaments while microtubules were stained using an antibody to β-tubulin following exposure to the most promising compound identified in initial screens (**11**) alongside CA4P and colchicine.

In vehicle treated controls, microtubules originate from the centrosome and radiate to the edge of the cell (Figure 4, A), whereas actin filaments are mostly pericellular (Figure 4, B). Upon treatment with 0.5 μM CA4P for 30 minutes, microtubules became disrupted (Figure 4, C), resulting in changes to cellular morphology as we have shown before.[35,37] Disruption of microtubules resulted in the formation of actin stress fibres across the cells (Figure 4, D). Colchicine was slower acting than CA4P, with a 30 minute treatment resulting in contraction of the cells (Figure 4, E and F). Many microtubules remained intact at this time point. A longer treatment of 90 minutes afforded results that resembled a 30 minute treatment with CA4P (Figure 4, G and H). At concentrations of 0.5 μM, **11** instigated similar levels of microtubule disruption and morphological changes to CA4P (Figure 4, I). There was also clear formation of actin stress fibres (Figure 4, J). With evidence that **11** could instigate tubulin depolymerisation, we sought to further probe the action of this compound.

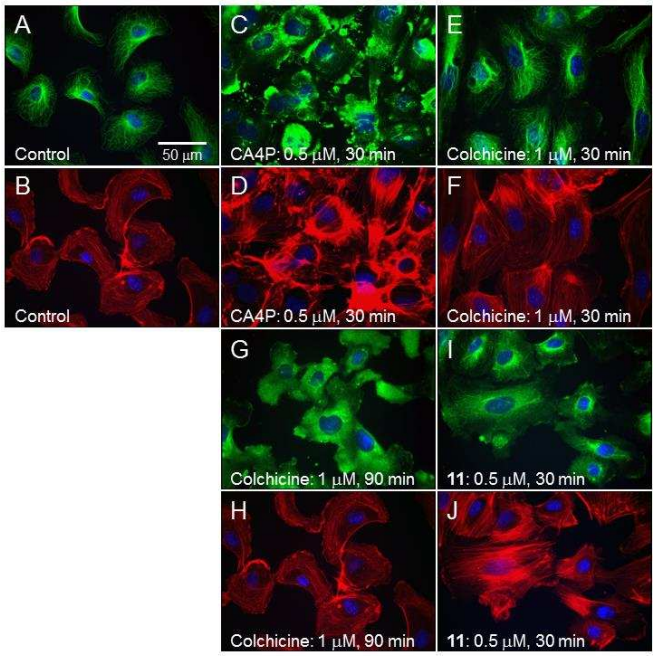

Figure 4. Drug effects on HUVEC cytoskeletal structures. Cells were treated with a single dose of either vehicle (A, B), 500 nM CA4P (C, D), 1 μM colchicine (E, F, G, H), 0.5 μM drug **11** (I, J). Drug treatments were for 30 min with CA4P (C, D), colchicine (E, F) and drug **11** (I, J) and 90 minutes with colchicine (G, H). Cells were fixed and stained with an antibody to β-tubulin (A, C, E, G, I) and F-actin (B, D, F, H, J).

Recovery Experiments

The lower toxicity of CA4P relative to colchicine is thought to be due to the differences in the reversibility of binding to tubulin.[39] Colchicine is thought to bind strongly and irreversibly, whereas CA4P appears to bind reversibly. Therefore, we tested the reversibility of the binding of **11** to tubulin using immunofluorescence in parallel with both CA4P and colchicine. As shown above, thirty minutes treatment with 0.5 μM CA4P or **11** resulted in marked changes in cellular morphology (*Figure 4*). Significant recovery of microtubules and a reduction in actin stress fibres was observed when the cells were allowed sixty minutes to recover after removal of CA4P (Figure 5, A and B). In contrast, cells treated for thirty minutes with colchicine, followed by removal of the drug and sixty minutes incubation drug-free did not show any signs of recovery (Figure 5, C and D). With CA4P and colchicine exhibiting a marked difference in recovery profile, we next sought to identify if **11** was a reversible tubulin binder. Pleasingly, allowing the cells sixty minutes recuperation after a thirty minute treatment with **11** led to significant recovery of cellular structure and microtubules (Figure 5, E and F). This was indicative of reversible binding, similar to that of CA4P, and provided evidence of a similar mechanism of action. It also provided some indication that **11** would not suffer from the same toxicity profile as colchicine.

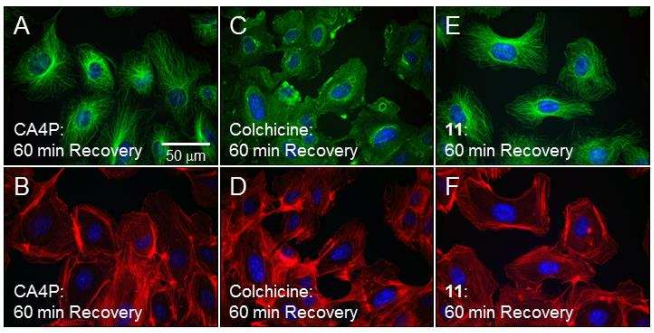

Figure 5. Recovery of cytoskeletal structures after drug removal. Cells were treated with a single dose of either 1 μM CA4P (A, B), 1 μM colchicine (C, D) or 1 μM drug **11** (E, F). Drug treatments were for 30 min. Cells were then washed with serum containing medium (3 x) and allowed to recover for 60 min. Cells were fixed and stained with an antibody to β-tubulin (A, C, E) and F-actin (B, D, F).

Endothelial Monolayer Permeability Experiments

The activity of VDAs stems from their ability to disrupt the endothelial cell monolayer of tumor blood vessels.[35] Therefore, in order to quantify this effect, studies in relation to cell monolayer permeability to fluorescent dextran were undertaken. Confluent HUVEC monolayers were treated for 30 minutes before removal of the drug and addition of the fluorescent dye for a further 30 minutes. The results showed that the addition of a 1 μM solution of both **11** and CA4P significantly increased the amount of fluorescent dye passing through the cell monolayer (Figure 6), indicating a clear increase in permeability.

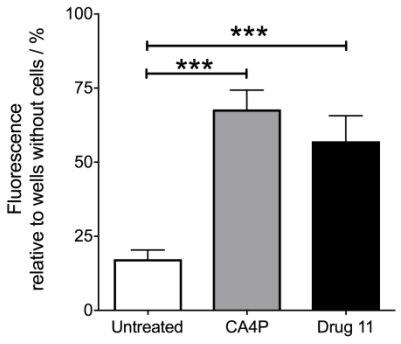

Figure 6. Drug-induced changes in endothelial monolayer permeability comparing CA4P and **11**. Confluent monolayers of cells grown on microporous filter inserts were treated with vehicle control, CA4P (1 μM, 30 min) or compound **11** (1 μM, 30 min). Drugs were removed and replaced with FITC – dextran for a further 30 min. The passage of FITC-dextran through the monolayer was quantified and expressed as a percentage of FITC that passed through a filter without cells. Results are a mean of 3 independent experiments ± SEM. *represents $P < 0.05$ for the significance of differences between groups (one-way ANOVA followed by a Tukey post-test).

Analysis of Rho-GTPase/Rho Kinase Signaling Pathway Activation

Next, we decided to examine whether **11** acted by triggering similar signalling pathways to those observed in CA4P. We have previously shown that activation of the RhoA-GTPase signal pathway was involved in actin remodelling caused by CA4P.[35] Actin polymerization and the phosphorylation of myosin light

chain (MLC) resulted in stress fiber formation. The activity was modulated by serine/threonine Rho kinases (ROCKs) The activation of the RhoA-ROCK pathway by CA4P was confirmed by increases in MLC phosphorylation upon exposure to the drug.[35] Therefore, we decided to investigate drug induced increases in the phosphorylation of MLC in HUVECs for both **11** and CA4P. It was found that both compounds instigated significant increases in the phosphorylation of MLC at various concentrations, indicating that both compounds were activating the same pathway (Figure 7). CA4P significantly increased levels of pMLC starting at 0.25 μM, however no effect was observed at 0.025 μM. Drug **11** was found to be slightly less active, failing to instigate increases in levels of pMLC at 0.25 μM. However, at 0.5 μM **11** instigated significant increases in pMLC.

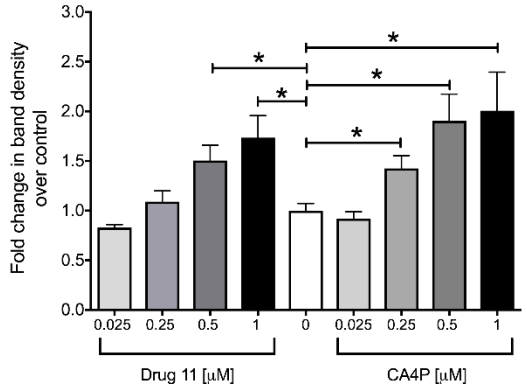

Figure 7. Drug-induced induction of phosphorylation of Rho kinase target MLC. HUVECs were treated with increasing concentrations of drug **11** or CA4P for 15 min after which proteins were extracted and analyzed for phosphorylation of ROCK target MLC (pMLC) by Western blotting using an antibody specific to the phosphorylated form of the protein (A). Immunoblots were reprobed with an antibody to actin to confirm equal loading. pMLC band intensities were analyzed by ImageJ and results expressed as fold-change over control cells treated with vehicle alone (B). Each column represents the mean of 3−4 independent cell culture experiments ± SEM. ∗represents $P < 0.05$ for the significance of differences between drug treatment groups and controls (paired Tukey post-test).

In order to further confirm that the phosphorylation of MLC was induced by activation of ROCK upon treatment with **11**, cells were treated with a specific ROCK inhibitor, Y-27632, before incubation with **11**. As was observed previously with CA4P,[35] drug **11**- and CA4P-induced phosphorylation of MLC was abrogated in the presence of Y-27632. Thus, confirming that ROCK is involved in the process.

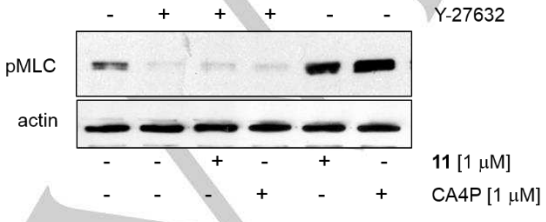

Figure 8. HUVECs were incubated with Rho kinase inhibitor Y-27632 (5 μM) for 5 min and then treated with 1 μM CA4P or **11** for 15 min. Proteins were extracted and analyzed for pMLC by Western blotting using an antibody specific to the phosphorylated form of the protein.

In Vivo Studies

To validate the results observed *in vitro*, experiments were undertaken to determine the activity of the drug *in vivo*. Due to the limited solubility of **11** in PBS, it was derivatized to the disodium phosphate compound **23** for *in vivo* studies. The maximum tolerated dose (MTD) of **23** in SCID (severe combined immunodeficiency) mice was found to be greater than 339 mg/kg (0.681 mmol/kg; data not shown). We next investigated whether **23** showed efficacy in a tumor model. SCID mice were implanted with 5 x 10^6 SW1222 (human colorectal adenocarcinoma) cells *via* subcutaneous injection. Tumors were allowed to reach 8 mm in diameter and then treated with either vehicle (50% Na_2CO_3/NaCl), CA4P (100 mg/kg, 0.227 mmol/kg) or a solution of **23** (339 mg/kg, 0.681 mmol/kg). Tumors were excised 24 hours later and necrosis levels calculated in H&E stained 5 μm thick sections by a random point scoring microscopy method using a 'Chalkley' eyepiece graticule.[40,41] As shown in Figure 9, CA4P treated tumors were significantly more necrotic than the untreated tumors, However, treatment with **23** did not have an effect on tumor necrosis. Such a lack of response to **23** indicated that the compound may not have reached the tumor blood vessels and was either metabolized before it could act or it was rapidly excreted. Only limited examples of mesoionic compounds have been tested *in vivo*[42,43] and their unusual structure makes it difficult to predict their pharmacokinetic profile and stability in the body. Nonetheless, this class of heterocycle has been a popular target in medicinal chemistry over several years, and the establishment of a viable administration route is therefore an important issue to address in the field. Further advances in this area are the subject of active investigation.[47, 48]

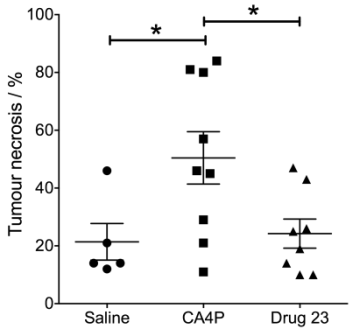

Figure 9. *In Vivo* Study of Drug-Induced effects on Tumor Cell Necrosis Comparing CA4P and **23**. Each point represents the combined data from a single tumor. 5 sections (cut at different tumor depths) were analyzed per tumor using a x20 objective on a Nikon Eclipse TS100 microscope. The total section was analyzed and % necrosis calculated in each field from the relative number of points in a Chalkley eyepiece graticule co-incident with necrotic versus viable tumor tissue. Bars represent the mean±SEM of the combined data for each tumor. *represents $P < 0.05$ for the significance of differences between groups (one-way ANOVA followed by a Tukey post-test).

Conclusions

We have successfully prepared a range of diarylsydnones and tested their potential as tubulin binders *in vitro*. The most potent compound in the initial screen, **11**, showed promising activity and was shown to disrupt microtubules and affect cellular morphology at sub-micromolar levels. Its binding to tubulin was shown to be reversible, in a similar manner to combretastatin A4. Like CA4P, **11** also significantly increased endothelial cell monolayer permeability. The compound was derivatized to the corresponding phosphate salt **23**, but did not exhibit efficacy *in vivo*, possibly due to rapid metabolism. Further investigations are required on the stability of sydnones in animals to establish if the motif is viable for future therapeutics.

Experimental Section

General. ^{1}H NMR spectra were recorded on a Bruker AVIII HD 400 (400 MHz), Bruker AVI 400 (400 MHz), or DPX-400 (400 MHz) supported by an Aspect 3000 data system. Chemical shifts are reported in parts per million (ppm) from tetramethylsilane with the residual protic solvent resonance as the internal standard ($CHCl_3$, δ 7.26; DMSO, δ 2.50). ^{13}C NMR spectra were recorded on a Bruker AVIII HD 400 (100.6 MHz), Bruker AVI 400 (100.6 MHz), or DPX-400 (100.6 MHz) with complete proton decoupling. Chemical shifts are reported in ppm from tetramethylsilane with the solvent as the internal reference ($CDCl_3$, δ 77.16; DMSO-d^6, δ 39.52). High-resolution mass spectra (HRMS), recorded for accurate mass analysis, were obtained in electrospray mode (TOF ES+). Infrared (IR) spectra were recorded on a PerkinElmer Paragon 100 FTIR spectrophotometer, ν_{max} in cm^{-1}. Samples were recorded as solids using a solid probe. Bands were characterized as broad (br), strong (s), medium (m), and weak (w). Flash chromatography was performed on silica gel (BDH silica gel 60 43-60). Thin layer chromatography (TLC) was performed on aluminum backed plates precoated with silica (0.2 mm, Merck DCalufolien Kieselgel 60 F254) which were developed using ultraviolet (UV). All compounds submitted for biological testing were recrystallized to consistent melting point and judged as >95% pure by ^{1}H and ^{13}C NMR spectroscopy unless otherwise specified. Sydnones were prepared by standard methods (cyclodehydration of *N*-nitroso amino acid with trifluoroacetic anhydride).[36]

General Procedure for the Direct Arylation of Sydnones. A mixture of sydnone (1 eq.), aryl halide (1.5 eq.), palladium acetate (5 mol %), XPhos (10 mol %) and potassium carbonate (2-3 eq.) in DMF (0.1 – 0.5 M) under an atmosphere of nitrogen was heated at 80 - 120 °C for 14 hours before the reaction was allowed to cool to ambient temperature and water was added. The resulting mixture was extracted with ethyl acetate:40-60 petroleum ether (9:1) and the combined organic layers dried over $MgSO_4$ and concentrated *in vacuo*. Flash silica chromatography (eluting solvent 20%-100% ethyl acetate in 40-60 petroleum ether) afforded the target 3,4-disubstituted sydnones. The compounds could be further purified by recrystallization from ethanol or dichloromethane/petrol.

4-(4-Methoxyphenyl)-*N*-(3,4,5-trimethoxyphenyl)sydnone (1). *N*-(3,4,5-Trimethoxyphenyl)sydnone (114 mg, 0.452 mmol) and 4-chloroanisole (97 mg, 0.68 mmol) were subjected to the general conditions affording **1** as colourless crystals (119 mg, 73%). M.p.: 165-167 °C (dec.); ^{1}H NMR (400 MHz, $CDCl_3$): δ 3.78 (6H, s), 3.79 (3H, s), 3.92 (3H, s), 6.67 (2H, s), 6.82 – 6.88 (2H, m), 7.27 – 7.31 (2H, m); ^{13}C NMR (101 MHz, $CDCl_3$): δ 55.4, 56.6, 61.2, 102.5, 108.0, 114.3, 116.8, 128.9, 129.9, 140.6, 154.1, 159.9, 167.2; FTIR: ν_{max} 2945 (w), 1723 (m), 1604 (s), 1232 (s), 1121 (s), 1019 (s), 987 (s); HRMS calculated for $C_{18}H_{19}N_2O_6$ (ES^+)($+H^+$): 359.1243. Found: 359.1226.

4-(2-Methoxyphenyl)-*N*-(3,4,5-trimethoxyphenyl)sydnone (2). *N*-(3,4,5-Trimethoxyphenyl)sydnone (200 mg, 0.792 mmol) and 2-bromoanisole (223 mg, 1.19 mmol) were subjected to the general conditions affording **2** as a colourless solid (202 mg, 71%). M.p.: 180-181 °C (dec.); ^{1}H NMR (400 MHz, $CDCl_3$): δ 3.40 (3H, s), 3.66 (6H, s), 3.84 (3H, s), 6.60 (2H, s), 6.78 (1H, dd, *J* = 8.5, 1.5 Hz), 7.03 (1H, td, *J* = 7.5, 1.0 Hz), 7.36 (1H, ddd, *J* = 8.5, 7.5, 1.5 Hz), 7.44 (1H, dd, *J* = 7.5, 1.5 Hz). ^{13}C NMR (101 MHz, $CDCl_3$): δ 55.1, 56.4, 61.2, 100.6, 105.3, 111.3, 114.0, 121.4, 131.3, 131.4, 131.7, 140.2, 153.6, 156.9, 167.8; FTIR: ν_{max} 2941 (b), 2837 (s), 1731 (s), 1607 (m), 1238 (s), 1120 (s), HRMS calculated for $C_{18}H_{19}N_2O_6$ (ES^+)($+H^+$): 359.1243. Found: 359.1226.

4-Phenyl-*N*-(3,4,5-trimethoxyphenyl)sydnone (3). *N*-(3,4,5-Trimethoxyphenyl)sydnone (99 mg, 0.39 mmol) and chlorobenzene (66 mg, 0.59 mmol) were subjected to the general conditions affording **3** as a tan solid (124 mg, 81%). M.p.: 146-147 °C (dec.); ^{1}H NMR (400 MHz, $CDCl_3$): δ 3.77 (6H, s), 3.93 (3H, s), 6.69 (2H, s), 7.28-7.39 (5H, m); ^{13}C NMR (101 MHz, $CDCl_3$): δ 56.6, 61.3, 102.4, 107.8, 124.6, 127.4, 128.8, 128.9, 129.9, 140.8, 154.1, 167.1; FTIR: ν_{max} 2945 (w), 1746 (s), 1603 (s), 1232 (s), 1125 (s), 977 (s); HRMS calculated for $C_{17}H_{17}N_2O_5$ (ES^+)($+H^+$): 329.1137. Found: 329.1125.

4-(4-Tolyl)-*N*-(3,4,5-trimethoxyphenyl)sydnone (4).[30] *N*-(3,4,5-Trimethoxyphenyl)sydnone (151 mg, 0.599 mmol) and 4-chlorotoluene (114 mg, 0.901 mmol) were subjected to the general conditions affording **4** as colourless crystals (196 mg, 96%). M.p.: 140-141 °C (dec.) (Lit.[30] 140–141 °C); ^{1}H NMR (400 MHz, $CDCl_3$) δ 2.31 (3H, s), 3.75 (6H, s), 3.91 (3H, s), 6.67 (2H, s), 7.10 (2H, d, *J* = 8.0 Hz), 7.22 (2H, d, *J* = 8.0 Hz); ^{13}C NMR (101 MHz, $CDCl_3$) δ 21.4, 56.6, 61.2, 102.5, 108.0, 121.7, 127.3, 129.5, 130.0, 139.0, 140.7, 154.1, 167.1; FTIR: ν_{max} 2942 (w), 2840 (w), 1749 (s), 1128 (s), 984 (m); HRMS calculated for $C_{18}H_{18}N_2O_5$ (TOF ES^+)($+H^+$): 343.1294. Found: 343.1283.

4-(3-Nitrophenyl)-*N*-(3,4,5-trimethoxyphenyl)sydnone (5). *N*-(3,4,5-Trimethoxyphenyl)sydnone (103 mg, 0.408 mmol) and 1-chloro-3-nitrobenzene (96 mg, 0.61 mmol) were subjected to the general conditions affording **5** as orange crystals (137 mg, 90%). M.p.: 148-149 °C; ^{1}H NMR (400 MHz, $CDCl_3$) δ 3.82 (6H, s), 3.95 (3H, s), 6.71 (2H, s), 7.52 (1H, td, *J* = 8.0, 1.0 Hz), 7.76-7.82 (1H, m), 8.08-8.15 (2H, m); ^{13}C NMR (101 MHz, $CDCl_3$) δ 56.8, 61.4, 102.6, 105.6, 121.1, 123.0, 126.5, 129.2, 129.9, 132.0, 141.5, 148.3, 154.6, 166.4; FTIR: ν_{max} 1748 (s), 1731 (s), 1605 (m), 1535 (s), 1352 (s), 1265 (s), 1230 (s), 1126 (s), 987 (m); HRMS calculated for $C_{17}H_{16}N_3O_7$ (ES^+)($+H^+$): 374.0988. Found: 374.0990.

4-(Thiophen-2-yl)-*N*-(3,4,5-trimethoxyphenyl)sydnone (6). *N*-(3,4,5-Trimethoxyphenyl)sydnone (103 mg, 0.410 mmol) and 2-chlorothiophene (73 mg, 0.62 mmol) were subjected to the general conditions affording **6** as yellow crystals (111 mg, 81%). M.p.: 173-174 °C; ^{1}H NMR (400 MHz, $CDCl_3$) δ 3.86 (6H, s), 3.96 (3H, s), 6.76 (2H, s), 7.00 (1H, dt, *J* = 5.0, 4.0 Hz), 7.26 (1H, dd, *J* = 5.0, 1.0 Hz), 7.39 (1H, dd, *J* = 4.0, 1.0 Hz); ^{13}C NMR (101 MHz, $CDCl_3$) δ 56.7, 61.4, 103.5, 106.5, 125.6, 126.2, 126.7, 127.5, 128.7, 141.3, 154.3, 165.7; FTIR: ν_{max} 3094 (w), 2943 (w), 2835 (w), 1746 (s), 1605 (m), 1235 (s), 1127 (s), 998 (w); HRMS calculated for $C_{15}H_{15}N_2O_5S$ (ES^+)($+H^+$): 335.0702. Found: 335.0704.

4-(4-Ethoxyphenyl)-*N*-(3,4,5-trimethoxyphenyl)sydnone (7). *N*-(3,4,5-Trimethoxyphenyl)sydnone (200 mg, 0.792 mmol) and 4-bromophenetole (239 mg, 1.19 mmol) were subjected to the general conditions affording **7** as a tan solid (272 mg, 92%). M.p.: 143-144 °C (dec.); ^{1}H NMR (400 MHz, $CDCl_3$) δ 1.40 (3H, t, *J* = 7.0 Hz), 3.78 (6H, s), 3.92 (3H, s), 4.01 (2H, q, *J* = 7.0 Hz), 6.67 (2H, s), 6.80-6.86 (2H, m), 7.24-7.30 (2H, m); ^{13}C NMR (101 MHz, $CDCl_3$) δ 14.8, 56.7, 61.3, 63.7, 102.5, 108.2, 114.9, 116.7, 129.0, 130.1, 140.7, 154.2, 159.4, 167.3; FTIR: ν_{max} 2985 (w), 2941 (w), 1749 (s), 1600 (m), 1231 (s), 1125 (s), 999 (m), 978 cm^{-1} (s); HRMS calculated for $C_{18}H_{19}N_2O_6$ (ES^+)($+H^+$): 373.1400. Found: 373.1408.

4-(2-Chlorophenyl)-*N*-(3,4,5-trimethoxyphenyl)sydnone (8). *N*-(3,4,5-Trimethoxyphenyl)sydnone (101 mg, 0.399 mmol) and 1,2-dichlorobenzene (88 mg, 0.60 mmol) were subjected to the general conditions affording **8** as a colourless solid (105 mg, 73%). M.p.: 135-136 °C; ^{1}H NMR (400 MHz, $CDCl_3$) δ 3.67 (6H, s), 3.85 (3H, s), 6.59 (2H, s), 7.29-7.45 (4H, m); ^{13}C NMR (101 MHz, $CDCl_3$) δ 56.4, 61.2, 101.2, 105.7, 124.3, 127.6, 129.9, 130.3, 131.7, 132.9, 135.7, 140.6, 153.7, 167.0; FTIR: ν_{max} 3058 (w), 2943 (w), 1757 (s), 1608 (m), 1234 (m), 1130 (s), 1049 (w), 988 (m); HRMS calculated for $C_{17}H_{16}{}^{[35]}ClN_2O_5$ (ES^+)($+H^+$): 363.0748. Found: 363.0736.

4-(3-Amino-4-methoxyphenyl)-*N*-(3,4,5-trimethoxyphenyl)sydnone (9). *N*-(3,4,5-Trimethoxyphenyl)sydnone (100 mg, 0.396 mmol) and 5-bromo-2-methoxyaniline (120 mg, 0.595 mmol) were subjected to the general conditions affording **9** as an orange solid (135 mg, 91%). M.p.: 173-174 °C; ^{1}H NMR (400 MHz, $CDCl_3$) δ 3.77 (6H, s), 3.80 (3H, s), 3.83 (2H, s), 3.90 (3H, s), 6.52 (1H, dd, *J* = 8.5, 2.0 Hz), 6.64 (1H, d, *J* = 8.5 Hz), 6.68 (2H, s), 6.85 (1H, d, *J* = 2.0 Hz); ^{13}C NMR (101 MHz, $CDCl_3$) δ 55.6, 56.6, 61.2, 102.5, 108.4, 110.2, 113.4, 117.1, 118.1, 130.1, 136.6, 140.5, 147.7, 154.0, 167.2; FTIR: ν_{max} 3471 (w), 3367 (w), 2941 (w), 2838 (w), 1732 (s), 1606 (m), 1224 (s), 1127 (s); HRMS calculated for $C_{18}H_{20}N_3O_6$ (ES^+)($+H^+$): 374.1352. Found: 374.1353.

4-(3-Hydroxy-4-methoxyphenyl)-*N*-(3,4,5-trimethoxyphenyl)sydnone (10). *N*-(3,4,5-Trimethoxyphenyl)sydnone (500 mg, 1.98 mmol) and 5-bromo-2-methoxyphenol (604 mg, 2.97 mmol) were subjected to the general conditions. Flash silica chromatography (eluting solvent 10%-30% ethyl acetate in dichloromethane) afforded **10** as a yellow solid (599 mg, 81%). M.p.: 237-239 °C (dec.); ^{1}H NMR (400 MHz, DMSO): δ 3.73 (9H, s), 3.76 (3H, s), 6.71 (1H, dd, *J* = 8.5, 2.0 Hz), 6.88 (1H, d, *J* = 2.0 Hz), 6.91 (1H, d, *J* = 8.5 Hz), 7.13 (2H, s), 9.28 (1H,s); ^{13}C NMR (101 MHz, DMSO): δ 55.5, 56.5, 60.4, 103.9, 108.1, 112.0, 114.1, 117.0, 118.5, 129.9, 139.8, 146.3, 148.1, 153.5, 166.2; FTIR: ν_{max} 3415 (br), 3062 (w), 2947 (w), 1718 (s), 1605 (m), 1243 (s), 1125 (s), 1014 (s), 949 (m); HRMS calculated for $C_{18}H_{19}N_2O_7$ (ES^+)($+H^+$): 375.1192. Found: 375.1192.

4-(3,4,5-Trimethoxyphenyl)-*N*-(3-hydroxy-4-methoxyphenyl)sydnone (11).[36] *N*-(3-Hydroxy-4-methoxyphenyl)sydnone (473 mg, 2.27 mmol) and 5-bromo-1,2,3-trimethoxybenzene (842 mg, 3.41 mmol) were subjected to the general conditions affording **11** as a colourless solid (402 mg, 47%). M.p.: 196-197 °C (Lit.[36] 196–197 °C); ^{1}H NMR (400 MHz, $CDCl_3$) δ 3.67 (6H, s), 3.83 (3H, s), 4.00 (3H, s), 5.94 (1H, s), 6.59 (2H, s), 6.92-7.05 (2H, m), 7.09 (1H, s); ^{13}C NMR (101 MHz, $CDCl_3$) δ 56.1, 56.5, 61.0, 104.7, 108.0, 111.0, 111.7, 117.2, 119.9, 127.8, 138.5, 147.0, 149.5, 153.3, 167.2; FTIR: ν_{max} 3295 (br), 3082 (w), 2940 (w), 2836 (w), 1710 (s), 1600 (w), 1581 (m), 1509 (s), 1229 (s), 1125 (s) 1014 (m), 998 (m); HRMS calculated for $C_{18}H_{19}N_2O_7$ (ES^+)($+H^+$): 375.1192. Found: 375.1181.

4-(3,4,5-Trimethoxyphenyl)-*N*-(4-ethoxyphenyl)sydnone (12). *N*-(4-Ethoxyphenyl)sydnone (102 mg, 0.494 mmol) and 5-bromo-1,2,3-trimethoxybenzene (149 mg, 0.741 mmol) were subjected to the general conditions affording **12** as colourless crystals (140 mg, 76%). M.p.: 129-130 °C (dec.); ^{1}H NMR (400 MHz, $CDCl_3$) δ 1.45 (3H, t, *J* = 7.0 Hz), 3.63 (6H, s), 3.80 (3H, s), 4.09 (2H, q, *J* = 7.0 Hz), 6.54 (2H, s), 6.98-7.08 (2H, m), 7.37-7.45 (2H, m); ^{13}C NMR (101 MHz, $CDCl_3$) δ 14.7, 56.0, 60.8, 64.4, 104.6, 107.8, 115.7, 120.0, 126.2, 127.1, 138.4, 153.3, 161.6, 166.8; FTIR: ν_{max} 2984 (w), 2937 (w), 2834 (w), 1743 (s), 1583 (m), 1250 (m), 1126 (s), 1046 (w), 1002 (w); HRMS calculated for $C_{19}H_{21}N_2O_6$ (ES^+)($+H^+$): 373.1400. Found: 373.1411.

4-(3,4,5-Trimethoxyphenyl)-*N*-(4-methoxyphenyl)sydnone (13). *N*-(4-Methoxyphenyl)sydnone (100 mg, 0.521 mmol) and 5-bromo-1,2,3-trimethoxybenzene (193 mg, 0.781 mmol) were subjected to the general conditions affording **13** as an yellow solid (132 mg, 71%). M.p.: 155-157 °C (dec.); ^{1}H NMR (400 MHz, $CDCl_3$): δ 3.65 (6H, s), 3.82 (3H, s), 3.89 (3H, s), 6.55 (2H, s), 7.03-7.10 (2H, m), 7.41-7.47 (2H, m). ^{13}C NMR (101 MHz, $CDCl_3$): δ 56.0, 56.1, 61.1, 104.2, 107.9, 115.3, 120.0, 126.6, 127.5, 138.5, 153.4, 162.3, 167.1. FTIR: ν_{max} 3116 (w), 3091 (w), 2944 (w), 2841 (w), 1729 (s), 1578 (s), 1125 (s), 991 (m); HRMS calculated for $C_{18}H_{19}N_2O_6$ (ES^+)($+H^+$): 359.1243. Found: 359.1239.

3,4-Bis(4-methoxyphenyl)sydnone (14).[30] *N*-(4-Methoxyphenyl)sydnone (1.00 g, 5.21 mmol) and 4-chloroanisole (0.99 g, 7.8 mmol) were subjected to the general conditions affording **14** as a tan solid (1.51 g, 97%). M.p.: 136-137 °C (dec.) (Lit.[30] 136–137 °C); ^{1}H NMR (400 MHz, $CDCl_3$) δ 3.78 (3H, s), 3.89 (3H, s), 6.79 – 6.86 (2H, m), 6.98 – 7.06 (2H, m), 7.20– 7.26 (2H, m), 7.35 – 7.43 (2H, m); ^{13}C NMR (101 MHz, $CDCl_3$) δ 55.4, 55.9, 108.0, 114.4, 115.2, 117.0, 126.3, 127.4, 129.0, 159.8, 162.1, 167.4.

4-Phenyl-*N*-(4-methoxyphenyl)sydnone (15).[30] *N*-(4-Methoxyphenyl)sydnone (105 mg, 0.547 mmol) and chlorobenzene (92 mg, 0.82 mmol) were subjected to the general conditions affording **14** as a pink solid (122 mg, 83%). M.p.: 106-107 °C (dec) (Lit.[30] 106-107 °C); ^{1}H NMR (400 MHz, $CDCl_3$) δ 3.89 (3H, s), 7.02 (2H, d, *J* = 9.0 Hz), 7.30 (5H, s), 7.39 (2H, d, *J* = 9.0 Hz); ^{13}C NMR (101 MHz, $CDCl_3$) δ 55.9, 107.8, 115.3, 124.8, 126.3, 127.4, 127.5, 128.7, 128.9, 162.2, 167.3.

4-(Thiophen-2-yl)-*N*-(4-methoxyphenyl)sydnone (16).[30] *N*-(4-Methoxyphenyl)sydnone (101 mg, 0.526 mmol) and 2-chlorothiophene (93 mg, 0.78 mmol) were subjected to the general conditions affording **16** as orange crystals (128 mg, 89%). M.p.: 129 °C (Lit.[30] 129 °C); ^{1}H NMR (400 MHz, $CDCl_3$) δ 3.93 (3H, s), 6.98 (1H, dt, *J* = 5.0, 4.0 Hz), 7.11 (2H, d, *J* = 9.0 Hz), 7.23 (1H, dd, *J* = 5.0, 1.0 Hz), 7.33 (1H, dd, *J* = 4.0, 1.0 Hz), 7.46 (2H, d, *J* = 9.0 Hz); ^{13}C NMR (101 MHz, $CDCl_3$) δ 57.0, 106.6, 115.4, 125.8, 126.1, 126.2, 126.4, 127.3, 127.5, 162.8, 165.9; FTIR: ν_{max} 3080 (w), 2941 (w), 2840 (w), 1756 (s), 1735 (s), 1176 (m), 1017 (s), 991 (m); HRMS calculated for $C_{13}H_{10}N_2O_3S$ (TOF ES^+)($+H^+$): 275.0490. Found: 275.0503.

4-(2-Chlorophenyl)-*N*-(4-methoxyphenyl)sydnone (17).[30] *N*-(4-Methoxyphenyl)sydnone (102 mg, 0.531 mmol) and 1,2-dichlorobenzene (117 mg, 0.796 mmol) were subjected to the general conditions affording **17** as an orange oil (151 mg, 94%). ^{1}H NMR (400 MHz, $CDCl_3$) δ 3.82 (3H, s), 6.91 (2H, d, *J* = 9.0 Hz), 7.27-7.40 (6H, m); ^{13}C NMR (101 MHz, $CDCl_3$) δ 55.8, 105.8, 115.0, 120.4, 124.0, 125.2, 127.5, 130.4, 131.5, 133.0, 135.4, 162.0, 167.2; FTIR: ν_{max} 3066 (w), 2936 (w), 2843 (w), 1757 (s), 1743 (s), 1028 (m), 1002 (m); HRMS calculated for $C_{15}H_{12}N_2O_3{}^{35}Cl$ (TOF ES^+)($+H^+$): 303.0536. Found: 303.0524.

4-(3-Nitrophenyl)-*N*-(4-methoxyphenyl)sydnone (18).[30] *N*-(4-Methoxyphenyl)sydnone (104 mg, 0.542 mmol) and 1-chloro-3-nitrobenzene (128 mg, 0.812 mmol) were subjected to the general conditions affording **18** as a yellow solid (144 mg, 85%). M.p.: 152-153 °C (dec.) (Lit.[30] 152-153 °C); ^{1}H NMR (400 MHz, $CDCl_3$) δ 3.92 (3H, s), 7.09 (2H, d, *J* = 9.0 Hz), 7.43 (2H, d, *J* = 9.0 Hz), 7.50 (1H, t, *J* = 8.0 Hz), 7.75 (1H, d, *J* = 8.0 Hz), 8.02-8.12 (2H, m); ^{13}C NMR (101 MHz, d_6-DMSO) δ 56.9, 106.5, 115.4, 121.2, 122.8, 126.5, 126.6, 127.1, 130.2, 132.8, 147.6, 161.9, 166.2.

4-(4-Tolyl)-*N*-(4-ethoxyphenyl)sydnone (19).[30] *N*-(4-Ethoxyphenyl)sydnone (127 mg, 0.616 mmol) and 4-chlorotoluene (117 mg, 0.924 mmol) were subjected to the general conditions affording **19** as a tan solid (140 mg, 77%). M.p.: 123-124 °C (dec.) (Lit.[30] 123-124 °C); ^{1}H NMR (400 MHz, $CDCl_3$) δ 1.45 (3H, t, *J* = 7.0 Hz), 2.29 (3H, s,), 4.09 (2H, q, *J* = 7.0 Hz), 6.94-7.02 (2H, m), 7.08 (2H, d, *J* = 8.0 Hz), 7.18 (2H, d, *J* = 8.0 Hz), 7.30-7.39 (2H, m); ^{13}C NMR (101 MHz, $CDCl_3$) δ 14.7, 21.4, 64.3, 108.0, 115.6, 121.9, 126.2, 127.2, 127.3 129.5, 138.8, 161.5, 167.3; FTIR: ν_{max} 2981 (w), 2934 (w), 1737 (s), 1115 (m), 1041 (m), 1002 (m); HRMS calculated for $C_{17}H_{16}N_2O_3$ (TOF ES^+)($+H^+$): 297.1239. Found: 297.1249.

4-(4-Tolyl)-*N*-phenylsydnone (20).[30] *N*-Phenylsydnone (102 mg, 0.629 mmol) and 4-chlorotoluene (119 mg, 0.940 mmol) were subjected to the

general conditions affording **20** as a tan solid (131 mg, 83%). M.p.: 134-136 °C (dec.) (Lit.[30] 141-143 °C) ^{1}H NMR (400 MHz, $CDCl_3$) δ 2.30 (3H, s), 7.08 (2H, d, *J* = 8.0 Hz), 7.16 (2H, d, *J* = 8.0 Hz), 7.47 (2H, d, *J* = 7.5 Hz), 7.57 (2H, t, *J* = 7.5 Hz), 7.60-7.70 (1H, m); ^{13}C NMR (101 MHz, $CDCl_3$) δ 21.4, 108.2, 121.6, 125.0, 127.4, 129.5, 130.2, 132.1, 134.8, 139.0, 167.3.

4-(3,4,5-Trimethoxyphenyl)-*N*-(3-*O*-phosphate[sodium salt]-4-methoxyphenyl)sydnone (23). To a suspension of **11** (73 mg, 0.20 mmol) in CH_2Cl_2 (1 mL) was added a solution of phosphorous oxychloride (179 mg, 1.17 mmol) in CH_2Cl_2 (1 mL) dropwise and the reaction stirred for one hour at room temperature. Triethylamine (47 mg, 0.47 mmol) was added and the reaction stirred at room temperature for 16 hours. Water was added and the reaction mixture extracted with CH_2Cl_2. Volatiles were removed *in vacuo*, and the crude material dissolved in a minimum of acetonitrile. Amberlite IR-120 Na^+ form (200 mg) in water was added and the reaction stirred at room temperature for 16 hours. The mixture was filtered and volatiles removed *in vacuo*. The resulting solid was recrystallized from acetone affording **23** as a yellow solid (78 mg, 80%). N.B. the compound was contaminated with a small amount of inseparable trisodium phosphate. ^{1}H NMR (400 MHz, D_2O) δ 3.69 (6H, s), 3.78 (3H, s), 3.94 (3H, s), 6.63 (2H, s), 7.24 (1H, d, *J* = 9.0 Hz), 7.32 (1H, app d, *J* = 9.0 Hz), 7.52 (1H, app s); ^{13}C NMR (101 MHz, D_2O) δ 56.0, 56.3, 60.9, 105.6, 109.5, 113.2, 118.0, 119.6, 121.7, 125.8, 137.4, 141.8 (d, *J* = 7.0 Hz), 152.6, 153.7 (d, *J* = 5.0 Hz), 168.8; ^{31}P NMR (162 MHz, D_2O) δ -4.32; FTIR: ν_{max} 3397 (br), 2949 (w), 1732 (s), 1580 (m), 1509 (s), 1283 (m), 1122 (s), 1109 (s), 946 (s); HRMS calculated for $C_{18}H_{17}N_2Na_2O_{10}P$ (TOF ES$^+$)(+H$^+$): 499.0494. Found: 499.0473.

2-Methoxy-5-((3,4,5-trimethoxyphenyl)ethynyl)phenol (22). A solution of **21** (8.05 g, 30.7 mmol), 1-bromo-3,4,5-trimethoxybenzene (5.05 g, 20.5 mmol), palladium acetate (0.09 g, 0.4 mmol) and triphenylphosphine (0.24 g, 0.8 mmol) in pyrollidine (60 mL) was heated at reflux for one hour. Aqueous NH_4Cl was added and the reaction mixture extracted with ethyl acetate. The organic phase was washed with aqueous HCl, dried over $MgSO_4$ and volatiles removed *in vacuo*. Flash silica chromatography (eluting solvent 40% ethyl acetate in 40-60 petroleum ether) afforded **22** as orange crystals (6.10 g, 95%). M.p. 97-99 °C (lit.[44] 97 °C); ^{1}H NMR (400 MHz, $CDCl_3$) δ 3.87 (3H, s), 3.88 (6H, s), 3.92 (3H, s), 5.62 (1H, s,), 6.75 (2H, s), 6.82 (1H, d, *J* = 8.5 Hz), 7.06 (1H, dd, *J* = 8.5, 2.0 Hz), 7.09 (1H, d, *J* = 2.0 Hz); ^{13}C NMR (101 MHz, $CDCl_3$) δ 55.2, 56.0, 61.0, 88.0, 88.5, 108.7, 110.6, 116.0, 117.6, 118.6, 124.3, 138.6, 145.4, 147.1, 153.1.

Biological Methods and Materials

Endothelial Cell Culture. Human Umbilical Vein Endothelial Cells (HUVECs) from pooled donors were purchased from Promocell GmbH (Promocell, C-12203) and cultured as we described before.[36] Briefly, cells were maintained for up to a maximum of six passages in endothelial cell basal medium (EBM) (Promocell, C-22010) supplemented with Endothelial Cell Growth Supplement Mix (Promocell, C-39215) and an extra 8% (v/v) low-endotoxin foetal calf serum (Invitrogen).

Immunofluorescence staining of the endothelial cytoskeleton. Changes in cell morphology and the cytoskeleton were visualised by dual staining of microtubules and actin filaments as we described previously.[35,36] Briefly, HUVECs were plated in Permanox Lab-Tek chamber slides (Life Technologies) coated with 5 μg/mL fibronectin and were allowed to reach confluence before they were exposed to drug or vehicle for 30 min. Cells were then fixed in 3.7% formalin in PBS and stained using an anti-β-tubulin antibody (Sigma, T4026) and Texas Red-X Phalloidin (Invitrogen, T7471). Cells were imaged using an Olympus BX microscope using Cell^F software. For analysis of 'recovery' of cytoskeletal structures, drug treated cells were washed several times with fresh medium containing serum and incubated at 37°C for up to 90 min as we described before.[36]

Cell Proliferation Studies. The effects of drugs on cell growth inhibition were established as we described previously.[36] HUVECs were plated in 96-multiwell plates (5 x 10^3 cells/well) and 24 h later they were treated with drug or vehicle. At 72 h after treatment cells were fixed and stained with 1% crystal violet (Sigma, Cat: C3886) solution in 10% ethanol. After several washes in PBS, the dye was solubilised in 10% acetic acid and absorbance was read at 590 nm. GI_{50} values were established for each drug using GraphPad Prism software.

Endothelial Monolayer Permeability Assay. Confluent HUVEC monolayers were established in fibronectin-coated (5 μg/mL) culture inserts (Falcon, 353492) set in companion 24-multiwell plates (Falcon, 353504) as described previously.[35,36] Drugs or vehicle were added directly to the cells within the inserts for 30 min before replacing the medium with fresh medium containing 0.8 mg/mL FITC-dextran (Sigma: 46945) and incubating the cells in this for a further 30 min. Fluorescence (excitation 488, emission 525) was quantified in samples of media taken from the lower well.

Analysis of pMLC phosphorylation by Western Blotting. Confluent HUVECs maintained in 12-multiwell plates were treated with drugs or vehicle for 20 min before proteins were extracted and analysed for MLC phosphorylation by western blotting using an antibody to dually phosphorylated MLC (Cell Signalling, # 3674) as described previously.[35,36] Blots were stripped and reprobed using an antibody to actin (Sigma, A4700).

***In Vivo* Analysis and Necrosis Scoring.** Animal experiments were conducted in accordance with the UK Animals (Scientific Procedure) Act 1986, with local ethics committee approval and following published guidelines for the use of animals in cancer research.[45] Female severe combined immunodeficiency (SCID) mice (8–12 weeks old, 20–25 g) were implanted subcutaneously into the rear dorsum with human colorectal adenocarcinoma SW1222 cells (5 × 10^6 cells in 0.05 mL) as described.[36,46] Once tumors reached approximately 8 mm in mean diameter animals were administered intraperitoneally with a single dose of either vehicle (50% Na_2CO_3/NaCl, 10 mL/kg), CA4P (100 mg/kg, 0.227 mmol/kg, in 50% Na_2CO_3/NaCl, 10 mL/kg) or a solution of **23** (339 mg/kg, 0.681 mmol/kg, 50% Na_2CO_3/NaCl, 10 mL/kg). Tumors were excised 24 hours after treatment and were formalin-fixed, paraffin-embedded, and hematoxylin and eosin (H & E) stained. The percentage of necrosis was quantified according to a random points scoring (Chalkley) system.[40]

Statistics. Statistical analysis was carried out using GraphPad Prism 6 for Windows 8.1. The significance of differences between groups was assessed using one-way ANOVA followed by a Tukey post-test, with $p<0.05$ considered significant.

Acknowledgements

The authors are grateful to Cancer Research UK and Yorkshire Cancer Research for financial support.

Keywords: Cancer • Palladium Catalysis • Sydnone • Tubulin Binders • Vascular Disrupting Agents

References:

[1] G. M. Tozer, C. Kanthou, B. C. Baguley, *Nat. Rev. Cancer* **2005**, *5*, 423-435.
[2] D. Neri, R. Bicknell, *Nat. Rev. Cancer* **2005**, *5*, 436-446.
[3] J. Folkman, *J. Nat. Cancer Institute* **1990**, *82*, 4-7.
[4] C. Kanthou, G. M. Tozer, *Expert Opin. Ther. Targets* **2007**, *11*, 1443-1457.

[5] J. Plowman, V. L. Narayanan, D. Dykes, E. Szarvasi, P. Briet, O. C. Yoder, K. D. Paull, Cancer Treatment Reports **1986**, *70*, 631-635.

[6] B. C. Baguley, W. R. Wilson, *Expert Rev. anticancer Ther.* **2002**, *2*, 593-603.

[7] E. Boyland, M. E. Boyland, *Biochem. J.* **1937**, *31*, 454-460.

[8] R. J. Ludford, *Br. J. Cancer* **1948**, *2*, 75-86.

[9] G. R. Pettit, G. M. Cragg, S. B. Singh, *J. Nat. Prod.* **1987**, *50*, 386-391.

[10] D. J. Chaplin, G. R. Pettit, C. S. Parkins, S. A. Hill, *Brit. J. Cancer Suppl.* **1996**, *27*, S86-S88.

[11] G. P. Kevin, R. P. George, T. MaryLynn, J. Christopher, J. C. David, in Anticancer Agents from Natural Products, Second Edition, CRC Press, 2011, pp 27-64.

[12] G. G. Dark, S. A. Hill, V. E. Prise, G. M. Tozer, G. R. Pettit, D. J. Chaplin, *Cancer Res.* **1997**, *57*, 1829-1834.

[13] G. R. Pettit, Combretastatin A-4 Prodrug, Google Patents, 1996.

[14] C. M. Lin, H. H. Ho, G. R. Pettit, E. Hamel, *Biochemistry* **1989**, *28*, 6984-6991.

[15] B. J. Monk, M. W. Sill, J. L. Walker, C. J. Darus, G. Sutton, K. S. Tewari, L. P. Martin, J. M. Schilder, R. L. Coleman, J. Balkissoon, C. Aghajanian, *J. Clin. Oncol.* **2016**, *34*, 2279-2286.

[16] R. Grisham, B. Ky, K. S. Tewari, D. J. Chaplin, J. Walker, *Gynecol. Oncology Res. Pract.,* **2018**, 5, 1.

[17] M. Cushman, D. Nagarathnam, D. Gopal, A. K. Chakraborti, C. M. Lin, E. Hamel, *J. Med. Chem.* **1991**, *34*, 2579-2588.

[18] K. Ohsumi, T. Hatanaka, K. Fujita, R. Nakagawa, Y. Fukuda, Y. Nihei, Y. Suga, Y. Morinaga, Y. Akiyama, T. Tsuji, *Bioorg. Med. Chem. Lett.* **1998**, *8*, 3153-3158.

[19] R. Romagnoli, P. G. Baraldi, A. Brancale, A. Ricci, E. Hamel, R. Bortolozzi, G. Basso, G. Viola, *J. Med. Chem.* **2011**, *54*, 5144-5153.

[20] R. Romagnoli, P. G. Baraldi, O. Cruz-Lopez, C. Lopez Cara, M. D. Carrion, A. Brancale, E. Hamel, L. Chen, R. Bortolozzi, G. Basso, G. Viola, *J. Med. Chem.* **2010**, *53*, 4248-4258.

[21] H. Zhou, R. R. Hallac, R. Lopez, R. Denney, M. T. MacDonough, L. Li, L. Liu, E. E. Graves, M. L. Trawick, K. G. Pinney, R. P. Mason, *Am. J. Nucl. Med. Mol. Imag.* **2015**, *5*, 143-153.

[22] R. Zaninetti, S. V. Cortese, S. Aprile, A. Massarotti, P. L. Canonico, G. Sorba, G. Grosa, A. A. Genazzani, T. Pirali, *ChemMedChem* **2013**, *8*, 633-643.

[23] M. B. Hadimani, M. T. MacDonough, A. Ghatak, T. E. Strecker, R. Lopez, M. Sriram, B. L. Nguyen, J. J. Hall, R. J. Kessler, A. R. Shirali, L. Liu, C. M. Garner, G. R. Pettit, E. Hamel, D. J. Chaplin, R. P. Mason, M. L. Trawick, K. G. Pinney, *J. Nat. Prod.* **2013**, *76*, 1668-1678.

[24] E.-K. Jung, E. Leung, D. Barker, *Bioorg. Med. Chem. Lett.* **2016**, *26*, 3001-3005.

[25] D. L. Browne, J. P. A. Harrity, *Tetrahedron* **2010**, *66*, 553-568.

[26] D. L. Browne, M. D. Helm, A. Plant, J. P. A. Harrity, *Angew. Chem. Int. Ed.* **2007**, *46*, 8656-8658.

[27] D. L. Browne, J. F. Vivat, A. Plant, E. Gomez-Bengoa, J. P. A. Harrity, *J. Am. Chem. Soc.* **2009**, *131*, 7762-7769.

[28] R. S. H. Foster, J.; Vivat, J. F.; Browne, D. L.; Harrity, J. P. A., *Org. Biomol. Chem.* **2009**, *7*, 4052-4056.

[29] J. Comas-Barceló, R. S. Foster, B. Fiser, E. Gomez-Bengoa, J. P. A. Harrity, *Chem. Eur. J.* **2015**, *21*, 3257-3263.

[30] A. W. Brown, J. P. A. Harrity, *J. Org. Chem.* **2015**, *80*, 2467-2472.

[31] M. Cushman, D. Nagarathnam, D. Gopal, H. M. He, C. M. Lin, E. Hamel, *J. Med. Chem.* **1992**, *35*, 2293-2306.

[32] K. Gaukroger, J. A. Hadfield, N. J. Lawrence, S. Nolan, A. T. McGown, *Org. Biomol. Chem.* **2003**, *1*, 3033-3037.

[33] G. C. Tron, T. Pirali, G. Sorba, F. Pagliai, S. Busacca, A. A. Genazzani, *J. Med. Chem.* **2006**, *49*, 3033-3044.

[34] S.-J. Lunt, S. Akerman, S. A. Hill, M. Fisher, V. J. Wright, C. C. Reyes-Aldasoro, G. M. Tozer, C. Kanthou, *Int. J. Cancer* **2011**, *129*, 1979-1989.

[35] C. Kanthou, G. M. Tozer, *Blood* **2002**, *99*, 2060-2069.

[36] A. W. Brown, M. Fisher, G. M. Tozer, C. Kanthou, J. P. A. Harrity, *J. Med. Chem.* **2016**, *59*, 9473-9488.

[37] S. M. Galbraith, D. J. Chaplin, F. Lee, M. R. Stratford, R. J. Locke, B. Vojnovic, G. M. Tozer, *Anticancer Res.* **2001**, *21*, 93-102.

[38] J. A. Hadfield, K. Gaukroger, N. Hirst, A. P. Weston, N. J. Lawrence, A. T. McGown, *Eur. J. Med. Chem.* **2005**, *40*, 529-541.

[39] A. T. McGown, B. W. Fox, *Anti-cancer Drug Design* **1989**, *3*, 249-254.

[40] H. W. Chalkley, *J. Nat. Cancer Inst.* **1943**, *4*, 47-53.

[41] L. J. Williams, D. Mukherjee, M. Fisher, C. C. Reyes-Aldasoro, S. Akerman, C. Kanthou, G. M. Tozer, *Brit. J. Pharmacol.* **2014**, *171*, 4902-4913.

[42] L. F. Galuppo, F. A. dos Reis Lívero, G. G. Martins, C. C. Cardoso, O. C. Beltrame, L. M. B. Klassen, A. V. d. S. Canuto, A. Echevarria, J. E. Q. Telles, G. Klassen, A. Acco, *Basic Clin. Pharmacol. Toxicol.* **2016**, *119*, 41-50.

[43] R. J. Anto, G. Kuttan, R. Kuttan, K. Sathyanarayana, M. N. A. Rao, *J. Clin. Biochem. Nutrition* **1994**, *17*, 73-80.

[44] F. Lara-Ochoa, G. Espinosa-Pérez, *Tetrahedron. Lett.*, **2007**, *48*, 7007-7010.

[45] P. Workman, E. O. Aboagye, F. Balkwill, A. Balmain, G. Bruder, D. J. Chaplin, J. A. Double, J. Everitt, D. A. H. Farningham, M. J. Glennie, L. R. Kelland, V. Robinson, I. J. Stratford, G. M. Tozer, S. Watson, S. R. Wedge, S. A. Eccles, *Br. J. Cancer*, **2010**, *102*, 1555-1577.

[46] L. J. Williams, D. Mukherjee, M. Fisher, C. C. Reyes-Aldasoro, S. Akerman, C. Kanthou, G. M. Tozer, *Br. J. Pharmacol.*, **2014**, *171*, 4902-4913.

[47] R. Chandrasekhar, M. J. Nanjan, *Mini Rev. Med. Chem.*, **2012**, *12*, 1359-1365.

[48] S. T. Asundaria, C. Pannecouque, E. De Clercq, C. T. Supuran, K. C. Patel, *Med. Chem. Res.*, **2013**, *22*, 5752-5763.

Entry for the Table of Contents

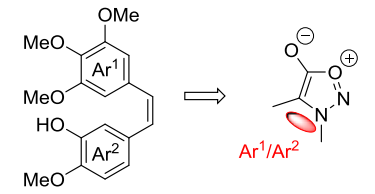

Combretastatin A4 Sydnone analogs

Cis is the answer! A family of novel configurationally fixed combretastatin analogs has been prepared that is based on a sydnone heterocycle core. The most potent analog was found to display tubular binding and disruption, and to affect cellular morphology and permeability in a similar manner to combretastatin A4.

WILEY-VCH